N···Br Halogen Bonding: One-Dimensional Infinite Chains through the Self-Assembly of Dibromotetrafluorobenzenes with Dipyridyl Derivatives**

Alessandra De Santis,[a] Alessandra Forni,[b] Rosalba Liantonio,[a] Pierangelo Metrangolo,*[a] Tullio Pilati,[b] and Giuseppe Resnati*[a]

Dedicated to Professor Francesco Minisci on the occasion of his 73rd birthday

Abstract: The N···Br halogen bonding drives the self-assembly of 1,4-dibromotetrafluorobenzene (**1a**) and its 1,3 or 1,2 analogues (**1b,c**, respectively) with dipyridyl derivatives **2a,b**. The isomeric supramolecular architectures **3a–f** are obtained as cocrystals that are stable in the air at room temperature. The solid-state features of these 1D infinite chains **3** have been fully characterized by single-crystal X-ray, Raman, and IR analyses. The occurrence of N···Br halogen bonding in solution has been detected with ^{19}F NMR spectroscopy. The N···Br halogen bonding is highly selective and directional and the geometry of the single strands of noncovalent copolymers **3** is programmed by the geometry of halogen-bonding donor and acceptor sites on the starting modules. The composition and topology of the instructed networks can be predicted with great accuracy. Experiments of competitive cocrystal formation established the strength of the N···Br interaction relative to other halogen bondings and the ability of different modules **1** to be involved in site-selective supramolecular syntheses.

Keywords: bromine · fluorine · halogen bonding · self-assembly · supramolecular chemistry

Introduction

Perfluorocarbon (PFC) derivatives have a unique set of physical and chemical properties compared with those of their hydrocarbon (HC) parents.[1] For instance, saturated PFCs are dense, highly inert liquids, with greater compressibilities and viscosities but lower internal pressures, refractive indexes, and surface tensions than their HC analogues. Aromatic PFCs and HCs have large quadrupolar moments that are similar in magnitude, yet opposite in sign.[2] Specifically tailored intermolecular interactions therefore have to be exploited if the PFC–HC recognition process is pursued to the point of triggering the self-assembly of the two species into cocrystals. Herein we describe how the N···Br–Ar_f attractive interaction (Ar_f = perfluoroaryl moiety) occurring between dibromo-PFCs **1a–c** and dipyridyl derivatives **2a,b** is specific, directional, and sufficiently strong to drive the self-assembly of PFC and HC modules into cocrystals **3a–f**, which are stable and solid at room temperature. Owing to the strength of the interaction, the overall features of the self-assembly process become largely independent from module structures.

A strong noncovalent interaction exists between heteroatoms possessing lone pairs, which work as electron-donor sites (Lewis bases, halogen-bonding acceptors), and halogen atoms, which work as electron acceptor sites (Lewis acids, halogen-bonding donors). To emphasize the similarity with the better known hydrogen bonding, the term "halogen bonding" has been suggested for such an interaction.[3] Numerous analytical techniques consistently show how in the solid, liquid, and gas phases the halogen bonds formed by chlorine, bromine, and iodine atoms have different strengths. The acidity scale I > Br > Cl is documented for halogens, interhalogens, pseudohalogens, and halogens bound to HC residues.[4] Here we show how this scale also holds when the iodine and bromine atoms are bound to PFC residues. The presence of the fluorine atoms dramatically increases the electron-acceptor ability of iodine and bromine nuclei, the N···Br interaction becomes sufficiently strong to drive the

[a] Dr. P. Metrangolo, Prof. Dr. G. Resnati, A. De Santis, Dr. R. Liantonio
The G. Natta Department of Chemistry, Materials, and Chemical Engineering, Polytechnic of Milan
7, via Mancinelli, 20131 Milan (Italy)
Fax: (+39) 02-2399-3080
E-mail: pierangelo.metrangolo@polimi.it, giuseppe.resnati@polimi.it

[b] Dr. A. Forni, Dr. T. Pilati
CNR - Institute of Molecular Science and Technology, University of Milan
19, via Golgi, 20133 Milan (Italy)

[**] Perfluorocarbon-Hydrocarbon Self-Assembly, Part 21. For Part 20 see: ref. [12c].

Supporting information for this article is available on the WWW under http://www.chemeurj.org or from the author.

DOI: 10.1002/chem.200204655

self-assembly of bromoperfluoroarenes with pyridyl derivatives, while parent bromoarenes do not undergo a similar self-assembly process.

Results and Discussion

When equimolar amounts of 1,4-dibromotetrafluorobenzene (**1a**) or its 1,3 or 1,2 analogues (**1b** and **1c**, respectively), are

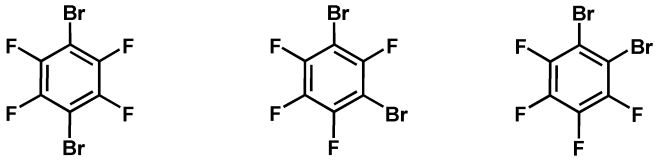

1a **1b** **1c**

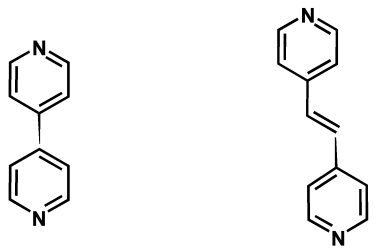

2a **2b**

crystallized with 4,4′-dipyridyl (**2a**), the noncovalent copolymers **3a**, **3c**, and **3e** are obtained in which the PFC and HC modules are present in a 1:1 ratio, and alternate in one-dimensional (1D) chains (Scheme 1).

1a + **2a** ⟶ ·····**1a**·····**2a**·····**1a**·····**2a**·····**1a**····· **(3a)**

1a + **2b** ⟶ ·····**1a**·····**2b**·····**1a**·····**2b**·····**1a**····· **(3b)**

1b + **2a** ⟶ ·····**1b**·····**2a**·····**1b**·····**2a**·····**1b**····· **(3c)**

1b + **2b** ⟶ ·····**1b**·····**2b**·····**1b**·····**2b**·····**1b**····· **(3d)**

1c + **2a** ⟶ ·····**1c**·····**2a**·····**1c**·····**2a**·····**1c**····· **(3e)**

1c + **2b** ⟶ ·····**1c,1c**·····**2b**·····**1c,1c**·····**2b**····· **(3f)**

Scheme 1. Formation and composition of cocrystals **3a–3f**.

Both **1a–c** and **2a** exhibit telechelic[5] behavior as the two bromine atoms of **1** and the two nitrogen atoms of **2** are involved in attractive N···Br halogen bondings, which pin the single modules in their positions in the formed 1D infinite chains **3**. Similarly, when 1,4- and 1,3-dibromotetrafluorobenzene (**1a,b**) are cocrystallized with (*E*)-1,2-bis(4-pyridyl)-ethylene (**2b**) the noncovalent copolymers **3b,d** are obtained where the PFC and HC modules are present in a 1:1 ratio. In these adducts, as in **3a,c,e**, the N···Br halogen bonding is reiterated at both bromine atoms of the PFC modules and both nitrogen atoms of the HC module. When 1,2-dibromotetrafluorobenzene (**1c**) is cocrystallized with **2b**, the 1D infinite network **3f** is formed in which the PFC and HC modules are held together by N···Br halogen bonds and are present in a 2:1 ratio. All adducts **3** are isolated as white solids, which are stable at room temperature and slowly lose, in air, the bromo-PFC module through sublimation. One-dimensional infinite chains structurally similar to noncovalent copolymers **3** are formed also when **2a,b** or other dipiridyl derivatives are cocrystallized with 1,4- and 1,2-diiodotetrafluorobenzene or with 1,4-diiodobenzene.[6] Also the iodo-PFCs sublime from the corresponding cocrystals, but this loss is much slower than that of bromo-PFCs from cocrystals **3**. This is consistent with the greater volatility of bromo-PFCs compared to the iodo-PFC analogues, and with the N···I interaction being stronger than the N···Br interaction (see below).

1,4-Dibromobenzene and its 1,3 and 1,2 analogues do not form cocrystals with **2a** and **2b**, the pyridyl modules invariably crystallizing in pure form independently from the employed solvent. The presence of electron-withdrawing groups on halocarbon modules is known to promote the acidity of the halogen atom, namely its tendency to be involved in strong halogen bonding.[4, 7] The fluorine-for-hydrogen substitution in dibromobenzenes boosts the ability of the bromine atoms to work as halogen-bonding donors to the point of making the supramolecular reactivity profile of Br-PFCs similar to that of I-HCs.

Melting point analyses and selective supramolecular syntheses: The melting points of all supramolecular architectures **3** are higher than those of pure PFC modules **1**. For some of these supramolecular architectures, they are also higher than those of pure HC modules **2**. The melting point of a substance depends on the intermolecular interaction strength and this dependence cannot be easily quantified due to the numerous parameters affecting the crystal packing. Nevertheless, useful qualitative information on the relative strength of the halogen bonding arising from different haloaromatics can be obtained by comparing the mean value of the melting points of the pure starting modules with the melting point of the corresponding cocrystals.

The melting point increase shown by iodo-PFCs containing cocrystals (Table 1, runs 15–17, 19) is invariably and dramatically greater than that shown by iodo-HCs containing cocrystals (runs 21 and 22) which, in turn, is slightly greater than that of bromo-PFCs containing cocrystals (runs 6–11, 13). The shortest contacts in all these cocrystals are those involving the nitrogen and halogen atoms, proving that the driving force of the self-assembly of the different modules is the halogen bonding. Haloarenes affording cocrystals with a greater melting point increase with respect to pure starting modules, and can be expected to give stronger halogen bondings. A scale of halogen-bonding donor ability can thus be written as I-PFCs $\gg$ I-HCs $\geq$ Br-PFCs, and this scale is consistent with experiments of competitive cocrystallization.

Table 1. Melting points of **1a–c**, **2a,b**, **3a–f**, and related bromo and iodo analogues.

Run	Compound	M. p. [°C][a]	M.p. mean value [°C][b]	ΔM.p. [°C][c]
1	**1a**	78–81 (A)		
2	**1b**	5–7 (B)		
3	**1c**	14–16 (B)		
4	**2a**	70–74 (C)		
5	**2b**	150–153 (C)		
6	**3a**	110–115 (C)	78	+36
7	**3b**	130–135 (C)	117	+18
8	**3c**	65–67 (C)	41	+26
9	**3d**	70–73 (C)	80	−7
10	**3e**	62–65 (C)	45	+20
11	**3f**	60–64 (C)	85	−19
12	1,2-BPE[d]	110–112 (C)		
13	**1a** · 1,2-BPE[d,e]	109–111 (D)	97	+14
14	1,4-DITFB[d]	108–110 (A)		
15	1,4-DITFB · **2a**[d,f]	180–182 (D)	92	+90
16	1,4-DITFB · **2b**[d,e]	236–240 (C)	132	+108
17	1,4-DITFB · 1,2-BPE[d,g]	204–207 (E)	111	+96
18	1,2-DITFB[d]	49–50 (A)		
19	1,2-DITFB · **2a**[d,h]	138–140 (C)	62	+78
20	1,4-DIB[d]	131–133 (A)		
21	1,4-DIB · **2a**[d,e]	147–149 (E)	104	+45
22	1,4-DIB · **2b**[d,e]	140–142 (E)	143	−1
23	1,4-DIB · 1,2-BPE[d]	145–147 (E)	123	+24

[a] Crystallization solvents: A: tetrachloromethane; B: neat; C: chloroform; D: acetone; E: dichloromethane. [b] Mean value of the starting modules melting points. [c] Difference between the melting point of the cocrystal and the mean value of the two starting modules melting points. [d] 1,2-BPE: 1,2-bis(4-pyridyl)ethane; 1,4-DITFB: 1,4-diiodotetrafluorobenzene; 1,2-DITFB: 1,2-diiodotetrafluorobenzene; 1,4-DIB: 1,4-diiodobenzene. [e] See ref. [6a]. [f] See ref. [6b]. [g] See ref. [6d]. [h] See ref. [6c].

When equimolar amounts of **2a**, **1a**, and 1,4-diiodotetrafluorobenzene are crystallized from chloroform, the cocrystal formed from **2a** and 1,4-diiodotetrafluorobenzene[6a] is isolated in pure form with up to a 90% recovery of **2a**, while **1a** remains in solution. Similarly, pure I-PFCs containing 1D infinite chains are obtained when **2b** competes with **1a** and 1,4-diiodotetrafluorobenzene, and when **2a** or **2b** compete with **1c** and 1,2-diiodotetrafluorobenzene. Selective formation of I-HCs containing cocrystals from solutions also containing Br-PFCs is also possible, but less easy. Crystallization of equimolar amounts of **2b**, **1a**, and 1,4-diiodobenzene affords, at a recovery of 30% of **2b**, a mixture of cocrystals containing preferentially 1,4-diiodobenzene. Two successive recrystallizations give the I-HC-containing infinite chain[6a] in pure form in approximately 4% overall yield.

Selective cocrystallizations also occur starting from mixtures of Br-PFCs. For instance, **3b** is obtained in pure form after one crystallization of equimolar solutions of **2b**, **1a**, and **1b**, or of **2b**, **1a**, and **1c**; **3e** is obtained in pure form after two consecutive crystallizations starting from an equimolar solution of **2a**, **1b**, and **1c**.

The ability of I-PFCs to form stronger halogen bonds than Br-PFCs has been also anticipated by quantum-mechanical calculations. According to the DFT method,[6a] the interaction dissociation energies of **2a** and **2b** with 1,4-diiodotetrafluorobenzene are 5.81 and 6.02 kcal mol^{-1}, respectively, and the interaction energy of 1,2-bis(4-pyridyl)ethane with **1a** is 3.65 kcal mol^{-1}. Similarly, the calculated interaction energy of ammonia with iodotrifluoromethane and bromotrifluoromethane is 7.1 and 5.0 kcal mol^{-1}, respectively.[8] These calculations correlate well with the experimental estimation of the intermolecular interaction energy.[6d]

Vibrational spectra properties: IR and Raman spectra of the infinite networks **3** are diagnostic of halogen-bonding formation and strength. The N···Br intermolecular interaction is weaker than covalent or ionic bonds, and it is reasonable to discuss vibrational spectra of adducts **3** in terms of modified modes of starting dibromo and dinitrogen modules **1** and **2**. The approach is typical for the determination of noncovalent adduct formation[9] and its validity is proven here by the consistency of the changes shown by different halogen-bonding donors when they interact with a variety of halogen-bonding acceptors. The bands shown by pure **1** and **2** are present in the spectra of the corresponding cocrystals **3** but the halogen bonding shifts some bands and/or changes their intensities.

In the IR spectra the ν_{CH} stretchings (3100–3000 cm^{-1} region) of HC modules **2** systematically shift to higher frequencies and decrease their intensities. These changes may be correlated with a decrease of the electron density on the pyridine ring. This is consistent with $n \rightarrow \sigma^*$ electron donation from the nitrogen to the bromine atoms.[10] Similar shifts to higher energy have been observed in other complexes in which single modules are held together by N···Br intermolecular interactions,[11] while similar but larger changes are observed when **2a,b** and other pyridyl derivatives interact with I-PFCs.[12] This is consistent with a greater electron donation from nitrogen to I-PFCs than to Br-PFCs and confirms that the former compounds are stronger halogen-bonding donors than the latter. When the Br-PFC modules **1** form halogen bonds to give the supramolecular architectures **3**, changes occur also in the absorbtions of the PFC module, for instance the stretchings of tetrafluorobenzene rings (1500–1460 cm^{-1} region) undergo red shifts ($\Delta\nu <$ 14 cm^{-1}).

Table 2 displays selected Raman absorptions. It can be seen that the pyridine ring absorptions of HC modules **2** at approximately 1000 cm^{-1} move to higher frequencies on the formation of N···Br interactions. Similar shifts have already been observed in IR and Raman spectra of related pyridine derivatives when the nitrogen atom was involved both in halogen and hydrogen bond formation.[12, 13] Br-PFCs containing cocrystals **3** give blue shifts similar to those given by I-HCs containing cocrystals and both these shifts are smaller than those given by I-PFCs containing cocrystals (Table 2), once again consistent with the acidity scale I-PFCs $\gg$ I-HCs $\geq$ Br-PFCs. Finally, some deformation bands of the PFC modules **1** (for example, the absorbtion at 211 cm^{-1} of **1a** and that at 270 cm^{-1} of **1c**) shift to lower frequencies on halogen-bonding formation so that with this technique the halogen-bonding formation can also be detected both on the PFC and the HC module.

X-ray structural analyses: The structural details of all the obtained halogen-bonded adducts **3** were established through single-crystal X-ray analyses at 90 K. Some selected crystallo-

Table 2. Selected Raman absorptions (neat, cm^{-1}) of **1a,c**, **2a,b**, **3a,b,e,f**, and related iodo analogues.

Compound	Absorptions[a]						
1a					211		
1c				270			
2a	1299	1001					
2b			996				
3a	1288	1003			208		
3b			998		208		
3e	1289	1002		267			
3f			996	266			
1,4-DITFB[b]							159
1,4-DITFB·**2a**[b]	1285	1008					152
1,4-DITFB·**2b**[b]			1001				149
1,2-DITFB[b]					235		
1,2-DITFB·**2a**[b]	1291	1005			227		
1,4-DIB[b]						159	
1,4-DIB·**2a**[b]	1287	1004				155	
1,4-DIB·**2b**[b]			997			155	

[a] Neat, cm^{-1}. [b] 1,4-DITFB: 1,4-diiodotetrafluorobenzene; 1,2-DITFB: 1,2-diiodotetrafluorobenzene; 1,4-DIB: 1,4-diiodobenzene.

graphic and data collection parameters are reported in Table 3 and some interesting structural parameters are listed in Table 4.

The most important short contacts present in **3a–f** are those involving nitrogen and bromine atoms. The N···Br distances range from 2.814(1) to 2.984(2) Å and are substantially shorter than the sum of the van der Waals radii for nitrogen (1.55) and bromine (1.85).[14] This proves the key relevance of the N···Br halogen bonding in driving the self-assembly of **1a–c** with **2a,b** to give the architectures **3a–f**. The shortening of the van der Waals distances between the halogen-bonded nuclei spans from 17 to 14%. The corresponding shortenings observed in the 1D infinite chains made up of **2a,b** and 1,4- or 1,2-diiodotetrafluorobenzenes are also reported in Table 4. Considering that the structures of the I-PFCs containing cocrystals have been collected at 294 K while the structures of Br-PFCs containing cocrystals have been collected at 90 K, it appears that the van der Waals radii shortenings of the former halogen-bonded systems are much greater than those of the latter. This difference in van der Waals radii shortenings is fully confirmed by the comparison between the structures of the 1D infinite chains that 1,2-bis(4-pyridyl)ethane gives with **1a**[6a] and with 1,4-diiodotetrafluorobenzene.[6d] Both these structures have been collected at 294 K and the shortening of the distances between the halogen-bonded nuclei are 11 and 21%, respectively. The shortening of van der Waals radii observed in I-HCs containing cocrystals is similar to that of cocrystals **3** and this further confirms that the halogen bonds associated with Br-PFCs are definitively weaker than those associated with I-PFCs and I-HCs, respectively.

Consistent with an $n \rightarrow \sigma^*$ electron donation from the nitrogen to the bromine atoms,[10] in all 1D infinite chains **3a–f** the halogen bonding develops on the extension of the C–Br bond with the C–Br···N angle varying between 162.52 and 179.12°. A similar directionality of the halogen bonding has been observed in I-PFCs and I-HCs containing infinite chains (Table 4). As a consequence, a lengthening of the C–Br and C–I bonds has been observed.[6e]

Except in the case of **3e**, some H···F distances shorter than the sum of proton and fluorine van der Waals radii are also present, but theoretical calculations on related systems

Table 3. Selected crystallographic and data collection parameters for cocrystal **3a–f**.

	3a	**3b**	**3c**	**3d**	**3e**	**3f**
molecular formula	$(C_{10}H_8N_2)\cdot(C_6Br_2F_4)$	$(C_{12}H_{10}N_2)\cdot(C_6Br_2F_4)$	$(C_{10}H_8N_2)\cdot(C_6Br_2F_4)$	$(C_{12}H_{10}N_2)\cdot(C_6Br_2F_4)$	$(C_{10}H_8N_2)\cdot(C_6Br_2F_4)$	$(C_{12}H_{10}N_2)\cdot 2(C_6Br_2F_4)$
M	464.06	490.10	464.06	490.10	464.06	797.98
crystal color	colorless	colorless	colorless	colorless	colorless	colorless
dimension [mm]	$0.33\times0.12\times0.09$	$0.21\times0.17\times0.14$	$0.20\times0.15\times0.12$	$0.39\times0.18\times0.14$	$0.20\times0.16\times0.10$	$0.38\times0.22\times0.16$
crystal system	triclinic	triclinic	monoclinic	monoclinic	monoclinic	monoclinic
space group	$P\bar{1}$	$P\bar{1}$	$P2_1/c$	$P2_1/c$	$P2_1/n$	$P2_1/c$
a [Å]	5.7752(3)	6.028(3)	5.7682(3)	7.8555(11)	9.0918(10)	9.842(2)
b [Å]	10.8979(6)	6.795(3)	34.8845(19)	5.9676(8)	8.3875(10)	7.9474(16)
c [Å]	12.1377(7)	11.062(5)	15.0566(8)	35.940(4)	20.313(2)	16.053(3)
α [°]	82.717(2)	83.099(12)				
β [°]	82.128(2)	86.459(12)	90.129(10)	94.927(4)	92.463(5)	98.43(3)
γ [°]	82.381(2)	68.625(12)				
V [Å^3]	745.43(7)	418.8(3)	3029.7(3)	1678.6(4)	1547.6(3)	1242.0(4)
Z	2	1	8	4	4	2
T [K]	90(2)	90(2)	90(2)	90(2)	90(2)	90(2)
ρ_{calcd} [g cm^{-1}]	2.068	1.943	2.035	1.939	1.992	2.134
μ ($Mo_{K\alpha}$) [mm^{-1}]	5.482	4.885	5.396	4.875	5.282	6.559
T_{min}, T_{max}	0.468, 0.607	0.435, 0.509	0.403, 0.523	0.395, 0.505	0.495,0.590	0.246, 0.350
$2\theta_{max}$ [°]	76.84	67.30	59.52	58.82	72.86	67.46
data collected	22153	5812	29890	13529	35982	17168
unique data, R_{int}	7964, 0.0271	3046, 0.0137	8019, 0.0320	4376, 0.0204	7288, 0.0422	4728, 0.0260
observed data [$I_o > 2\sigma(I_o)$]	6595	2843	6038	3896	5522	3843
no. parameters, no. restraints	249, 0	138, 0	481, 0	261, 33	249, 34	192, 0
R_{all}, R_{obs}	0.0339, 0.0261	0.0234, 0.0209	0.0511, 0.0333	0.0287, 0.0243	0.0547,0.0345	0.0360, 0.0239
wR_{all}, wR_{obs}	0.0647, 0.0628	0.0534, 0.0526	0.0796, 0.0753	0.0573, 0.0561	0.0751, 0.0694	0.0579, 0.0534
weighting [a], a,b	0.0367, 0.0000	0.0258, 0.1680	0.0348, 1.1762	0.0271, 0.2710	0.0352, 0.0000	0.0266, 0.3428
goodness-of-fit (restrained)	0.991	1.090	1.037	1.040	0.988	1.023
$\Delta\rho_{min,max}$ [e Å^{-3}]	−0.60, 1.17	−0.73,0.61	−0.63,0.74	−0.38, 0.50	−0.48,0.81	−0.39,0.59

[a] $w = 1/[\sigma^2(F_o)^2 + (aP)^2 + bP]$, where $P = (F_o^2 + 2F_c^2)/3$.

Table 4. Selected structural data of cocrystals **3a–f** and related bromo and iodo analogues.

Compound	N···X distance [Å]	van der Waals radii shortening [%]	C–X···N angle [°]	Temperature [K]
3a	2.878(1) 2.979(1)	14	177.71(4) 176.40(3)	90
3b	2.814(1)	17	179.11(4)	90
3c	2.987(2) 2.984(2) 2.868(2) 2.916(2)	14	179.12(9) 175.92(9) 163.90(9) 172.64(10)	90
3d	2.852(4) 2.913(5) 2.929(4) 2.989(4)	14	177.07(11) 177.36(11) 163.69(10) 169.22(9)	90
3e	2.880(2) 2.984(2)	14	170.89(5) 162.51(6)	90
3f	2.841(2)	16	174.29(5)	90
1,4-DITFB·**2a**[a,b]	2.864(2)	19	177.3(3)	290
1,2-DITFB·**2a**[a,c]	2.928(4) 2.909(5) 2.958(4) 2.964(5)	17	172.1(2) 175.5(2) 175.4(2) 176.2(2)	290
1,4-DITFB·**2b**[a,d]	2.810(5)	20	179.3(5)	294
1,4-DITFB·1,2-BPE[a,e]	2.79(5)	21	175.9(1)	294
1,4-DIB·**2a**[a,d]	3.032(3)	14	176.0(4)	294
1,4-DIB·**2b**[a,d]	2.996(3)	15	176.9(6)	294
1a·1,2-BPE[a,d]	3.025(9)	11	172.2(9)	294

[a] 1,4-DITFB: 1,4-diiodotetrafluorobenzene; 1,2-DITFB: 1,2-diiodotetrafluorobenzene; 1,2-BPE: 1,2-bis(4-pyridyl)ethane; 1,4-DIB: 1,4-diiodobenzene. [b] See ref. [6b]. [c] See ref. [6c]. [d] See ref. [6a]. [e] See ref. [6d].

predict they correspond to quite weak interactions (approximately 1 kcal mol^{-1}).[15] If the halogen bonding plays the fundamental role of driving the intermolecular recognition and self-assembly of the PFC and HC modules, the weaker interactions contribute to the structural cohesion of the crystal matrix in **3a–f**.

The unit cell of **3a** is formed by two half molecules of **1a** (molecules A and B) and two half molecules of **2a** (molecules C and D). The four molecules lie on four crystallographically distinct centers of symmetry so that both dipyridyl rings are planar. Due to the linear arrangement of the two bromine atoms in **1a**, of the two nitrogen atoms in **2a**, and of the halogen bonds, the 1D infinite chains **3a** assume a quite linear arrangement (Figure 1; in all figures, throughout the article

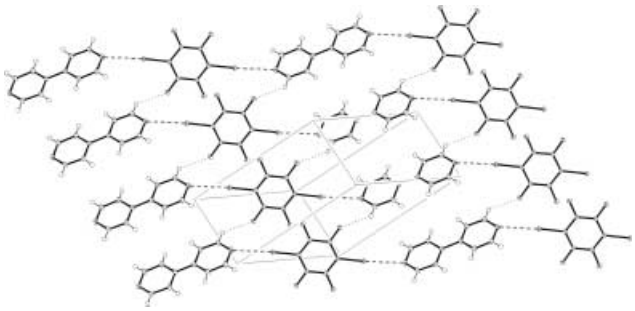

Figure 1. ORTEP view of a layer in the crystal structure **3a** including only chains formed by B and D modules.

and Supporting Information, atomic displacement parameters (ADPs) are at 50% of probability level, H atoms are not to scale, dashed lines represent the N···Br halogen bonds, dotted lines represent H···F hydrogen bonds). Two independent and parallel chains of alternating PFC and HC modules ···A···C···A···C··· and ···B···D···B···D··· are present in the cocrystal. These two distinct chains are very similar to each other and differ by the orientation that modules **1a** assume with respect to the adjacent modules **1b**; the dihedral angle between the least-square planes is 61.0° and 60.0° for the chains ···A···C···A···C··· and ···B···D···B···D···, respectively.

The asymmetric unit of **3b** consists of half a molecule of **1a** and half a molecule of **2b**. As a result, all the atoms of **2b** are coplanar. In the halogen-bonded infinite chain, the alternating PFC and HC modules are nearly coplanar; the dihedral angle between the least-square planes of the two modules is 4.2°. As in **3a**, the chains assume a quite linear arrangement (Figure 2) and weak H···F contacts bridge adjacent chains

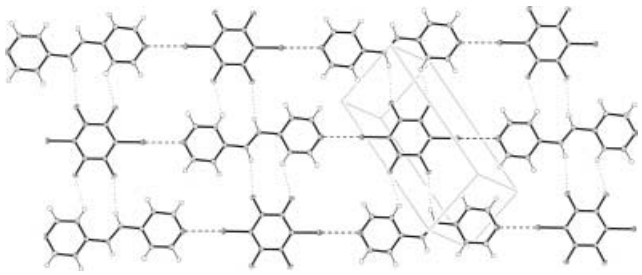

Figure 2. ORTEP view of a layer of the supramolecular architecture **3b**.

and arrange them in flat and loosely connected layers. A strictly similar packing of the modules has been observed in the cocrystal made up of **2b** and 1,4-diiodotetrafluorobenzene.[6a] This similarity confirms the predictability of the structure of halogen-bonding driven supramolecular architectures and the reliability of this intermolecular interaction in crystal engineering.

The cell of **3c** is quite complex. It contains two independent molecules of **1b**, while one molecule of **2a** occupies a general position and two others lie on a center of symmetry. As a result there are four distinct N···Br distances. The two pyridine rings in molecules **2a** lying on a center of symmetry are coplanar by symmetry, while in the other molecule the pyridine rings form an angle of 5.0°. Due to the 1,3 arrangement of the two bromine atoms in the module **1b**, any 1D infinite chain **3c** assumes a wavelike structure in which **1b** are the crests and **2a** are the walls (Figure 3). The dihedral angles between the least-square planes through the PFC module and the two adjacent pyridine rings are 54.8° and 60.0° (in the chain involving the dipyridyl molecules lying on the centers of symmetry), 57.7° and 55.6° (in the chain involving the other

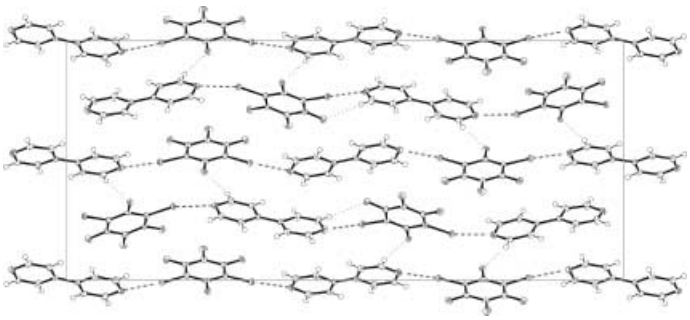

Figure 3. ORTEP view of crystal packing of **3c** viewed down the *a* axis.

dipyridyl molecule). Similar to **3a**, the infinite chains of **3c** form rippling surfaces.

The asymmetric unit of **3d** consists of one molecule of **1b** and one of **2b**. Module **2b** is disordered over two equally populated models related by a 180° symmetry about the internitrogen molecular axis. The two different N···Br interactions alternating in the 1D infinite network thus result in four values, two for each position assumed by the nitrogen atoms. One PFC and one HC module form couples of nearly coplanar modules (the dihedral angle between the least square planes through the disordered dipyridylethylene module and the dibromotetrafluorobenzene module is 3.8°). In the 1D infinite chains **3d**, two adjacent couples of coplanar modules are rotated with respect to each other, the dihedral angle being 54.0° (Figure 4). Moreover, in the crystal structure of **3d**, even if solved at 90 K, the dipyridile module is disordered as commonly shown by similar derivatives.[16]

The asymmetric unit of **3e** consists of two independent molecules, one of **1c** and one of **2a**. The two halogen bonds formed by any dibromobenzene modules **1c** are quite different (Table 4). The two pyridyl rings of **2a** are not coplanar and their least-square planes form an angle of 18.4°. The halogen-bonded infinite chains screw along a twofold axis (Figure 5). Any turn contains four modules, the dihedral angle between any dibrominated module and the two bonded dipyridyl moieties are 3.7 and 84.9°.

The asymmetric unit of **3f** contains a molecule of **1c** and half a molecule of **2b**. The dipyridylethylene module is on a center of symmetry and all its atoms are therefore coplanar. The distance between dibromobenzene rings related by a symmetry center is 3.447(4) Å, implying a $\pi-\pi$ attractive

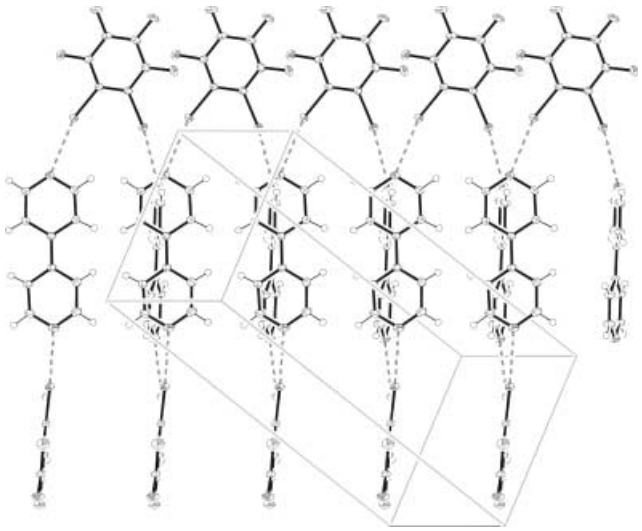

Figure 5. ORTEP view of a screw-shaped chain of **3e**.

interaction[2] that forms well-defined noncovalent dimers (Figure 6A). In these dimers, only one bromine atom per dibromobenzene module serves as a halogen-bonding donor towards the nitrogen atoms of **2b**, which behaves, like usual, as a bidentate halogen-bonding acceptor. The 1D infinite chain **3f** is thus formed (Figure 6B). In these chains the dimers of **1c** are bound to two dipyridylethylene modules through quite short N···Br distances, and the dihedral angle between **1c** and **2b** modules is 77.8°.

^{19}F NMR spectral changes: Br-PFCs also form halogen bonds in solution. ^{19}F NMR spectroscopy is a simple, powerful, and versatile tool to detect formation of the interaction in the liquid phase and to rank the electron donors and acceptors according to the strength of the halogen bonds they are involved in. Specifically, the signals of perfluoroalkyl and -aryl derivatives are shifted upfield when an interaction occurs and greater electron acceptor (or donor) abilities of the involved modules result in larger shifts.[17] In Table 5 the upfield shifts for **1a**, **1c**, and their diiodo analogues are reported. The chemical shift changes induced on **1a,c** by all the used halogen-bonding acceptors are significantly smaller than those induced on their diiodo analogues. Br-PFCs are weaker halogen-bonding donors than I-PFCs also in solution.

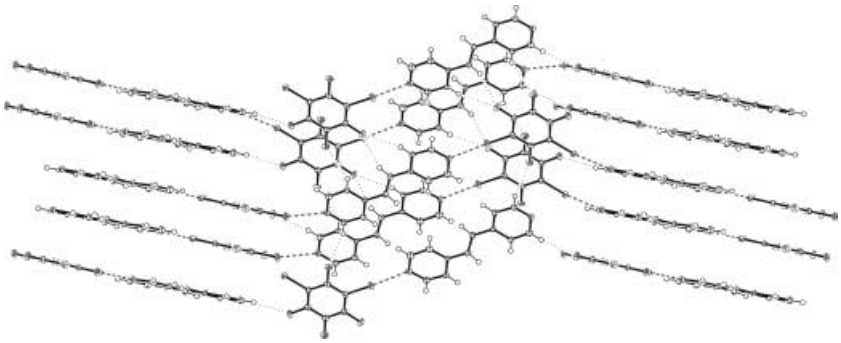

Figure 4. Partial view of **3d** packing. The figure highlights the arrangement of the 1D wavelike chains where a couple of coplanar **1b**···**2b** molecules are followed by a second coplanar pair rotated about 60° with respect to the first.

Conclusions

Transition metals (for example, palladium, platinum, zinc)[18] and organic proton donors (for example, phenols and carboxylic acids)[6d, 19] are the tectons[20] most frequently used to drive the self-assembly of polypyridyl derivatives into well-defined supramolecular architectures. The intermolecular interactions responsible for the

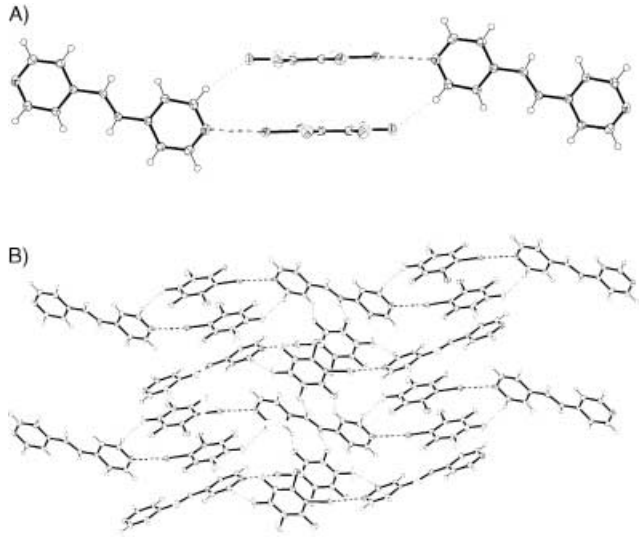

Figure 6. ORTEP views of **3f**. A) The basic structural element of the infinite chains is a unit formed by two dibromobenzene rings **1c** paired through the π – π interaction and connected to adjacent modules **2b** by two N···Br halogen bondings and two weak H···F hydrogen bonds. B) Arrangement of the basic structural units in A into the infinite chains.

recognition of single modules are metal coordination and hydrogen bonding, respectively. Here we have reported how N···Br halogen bonding drives the self-assembly of dibromoperfluorobenzenes **1** with dipyridyl derivatives **2** resulting in the formation of single-strand infinite chains **3**, which are isolated as solid cocrystals. Compounds **1** can thus be considered as new, effective, and reliable tectons for the formation of supramolecular architectures containing pyridyl derivatives. Some similarities exist in the supramolecular reactivity profiles of dibromotetrafluorobenzenes and of diiodotetrafluorobenzenes,[6] so that in general haloperfluoroarenes can be envisaged as useful tools at the disposal of the supramolecular chemist to drive the self-assembly of polypyridyl derivatives. The potential of the halogen bonding in crystal engineering is further extended.

The chain geometry in the noncovalent copolymers **3a**–**f** varies from the nearly perfect alignment of **3a** to the helical arrangement of **3e**. The self-assembly of the single strands of copolymers **3** is determined by the N···Br halogen bonding and the geometry of the strand is determined by the geometry of the halogen-bonding donor and acceptor sites on starting modules. For instance, when the "rod-type" module **2a** is paired with the "rod-type" module **1a**, the linear infinite chain **3a** is formed, and when **3a** is paired with the "angular-type" module **2b**, the zigzag chain of **3c** is generated. Similar chain geometry control based on the geometry of the modules used in the construction has been reported in metal coordination driven self-assembly of pyridyl derivatives.[18c]

Despite the topological diversity in **3a**–**f**, the geometrical parameters of the halogen bonding remain quite constant, the N···Br distances range from 2.814 to 2.984 Å and the N···Br–C angle varies between 162.52 and 179.12°. The N···Br halogen bonding is highly selective and directional so that the composition and topology of the instructed networks can be predicted with an accuracy that is unusual for crystal engineering. Several analytical techniques have been used to compare the strength of the N···Br–Ar_f interaction with the strength of other halogen bonds. While weaker than the N···I-Ar_f interaction, the N···Br–Ar_f interaction is invariant and sufficiently robust to drive effectively self-assembly processes, which are largely independent of the structure of the involved modules.

In solution the electron donation from amine and pyridine derivatives to bromine atoms bound to hydrocarbon chains has been studied with different analytical techniques.[3b, 21] Under photochemical conditions, the donation can evolve into an electron transfer process[22] confirming the rationalization of the halogen bonding as a pre-reactive state.[23]

The first example of N···Br–C halogen-bonding driven self-assembly involved tetrabromoethylene and pyrazine and was reported by Hassel as early as the late 1960s,[24] but only in a very few other cases was the recognition occurring in solution strong enough to drive the formation of cocrystals. Before our proposal of Br-PFCs as effective and reliable modules for the synthesis of two-component heteromeric architectures, only three other cocrystals had been described in which short N···Br–C interatomic distance are present.[21, 25] A search of the Cambridge Structural Database Database (CSD, version 5.23 April 2002, 257000 crystal structures) for short N···Br–C halogen bonds (≤3.20 Å)

Table 5. ^{19}F NMR chemical shift changes ($\Sigma\Delta\delta_F$)[a] given by **1a**, **1c** and their diiodo analogues moving from non basic (*n*-pentane) to basic solvents.[b]

Solvent	$\Sigma\Delta\delta_F$[a]			
	1a	1,4-DITFB[c]	**1c** (*ortho, meta*)	1,2-DITFB[c] (*ortho, meta*)
N-methylpiperidine	1.48	9.36	2.56 (1.42, 1.14)	14.42 (8.84, 5.58)
piperidine	3.32	14.40	4.34 (2.40, 1.94)	19.54 (11.52, 8.02)
cyclohexylamine	1.48	11.96	1.86 (1.32, 0.54)	16.1 (9.18, 6.92)
pyridine	1.28	7.68	1.54 (1.48, 0.06)	9.70 (6.46, 3.24)
4-methylpyridine	2.60	8.72	2.14 (1.76, 0.38)	10.70 (6.88, 3.82)
4-ethoxycarbonylpyridine	2.52	7.40	1.78 (1.58, 0.14)	8.32 (5.48, 2.84)

[a] $\Sigma\Delta\delta_F = \delta_F$ (in *n*-pentane used as a solvent) $- \delta_F$ (in the halogen-bonding acceptor used as a solvent); $\delta_{\mathbf{1a}\text{ in }n\text{-pentane}} = -132.89$, $\delta_{1,4\text{-DITFB in }n\text{-pentane}} = -119.44$; $\delta_{\mathbf{1c}\text{ in }n\text{-pentane}} = -125.44$ (*ortho*), -155.03 (*meta*); $\delta_{1,2\text{-DITFB in }n\text{-pentane}} = -104.88$ (*ortho*), -152.85 (*meta*). We report the overall chemical shift change for the molecule, namely the sum of the shift changes of each fluorine atom of the molecule. For instance, values reported in the column of **1a** are four times the chemical shift changes observed for the signal of 1,4-dibromotetrafluorobenzene, the values reported in the column of **1c** are two times the chemical shift changes observed for the signal of the fluorine in position 3 (*ortho* fluorine) plus two times the chemical shift changes observed for the signal of the fluorine in position 4 (*meta* fluorine). [b] Under the same experimental conditions hexafluorobenzene shows definitively smaller $\Sigma\Delta\delta_F$ values, confirming that the reported chemical shift changes are due to specific solute–solvent interactions rather than a non specific solvent effect. [c] 1,4-DITFB: 1,4-diiodotetrafluorobenzene; 1,2-DITFB: 1,2-diiodotetrafluorobenzene.

occurring in one-component crystals, shows that these bromine atoms are typically bound to electron-poor carbon moieties, for example cyanoalkynes and arenes.[26] These results are consistent with the fact that common organic bromides are poor halogen-bonding donors and only when the bromine atom is bound to strongly electron-withdrawing carbon moieties[4] is the Lewis acidity of the halogen boosted to the point that the N···Br–C interaction becomes strong enough to effectively drive recognition processes. The high electronegativity of fluorine thus accounts for the effectiveness of dibromoperfluorobenzenes **1** as tectons.[27]

The implications of the results reported here are far reaching and can be envisaged in all the fields in which recognition and self-assembly play a key role, from material science to biopharmacology. Br-PFCs being a class of compounds of high technological relevance,[28] the adducts obtained through their self-assembly with HC derivatives may have useful properties. For instance, due to the high vapor pressures of Br-PFCs, the modules **1** easily sublime off the adducts **3**. The removal of the Br-PFC module from the crystal matrix of PFC-HC adducts may develop into a general strategy to study polymorph interconversion or to obtain porous materials. This strategy may be complementary to that based on the removal of the halogen-bonding donor from cocrystals self-assembled by N···I interactions.[29] It may be even more effective as the N···Br interaction is weaker than the N···I interaction. Halotane (1-bromo-1-chloro-2,2,2-trifluorothane) is a commonly employed volatile anaesthetic, its two enantiomers have shown different pharmacological activity,[30] and the eudismic ratio has been attributed to the binding with a proteinaceous receptor site.[31] The enantioselective recognition of the drug in vivo may be mediated by the formation of a halogen-bonded complex between the bromine atom of halotane and a nitrogen atom of the peptide receptor. Similarly, the resolution of the racemic drug may be pursued through the diastereoselective formation of halogen-bonded adducts with enantiopure HC resolving agents.[32]

Experimental Section

General methods: All materials were obtained from commercial suppliers (Apollo Scientific and Aldrich) and were used without further purification. Redox S.n.c., Cologno Monzese, Milan, Italy performed elemental analyses. $^{1}H/^{19}F$ NMR spectra were recorded on a Bruker AV500 or a Bruker AC250 spectrometer at 25 °C. $CDCl_3$ was used as solvent, tetramethylsilane and $CFCl_3$ were used as internal standards. The expected signals of starting modules **1** and **2** were always observed in the cocrystals **3**, minor chemical shift changes were attributed to the presence of the halogen bonding. IR and Raman spectra were recorded with a Perkin-Elmer 2000 FT-IR and a Bruker FRA106 spectrophotometer, respectively. Selected IR, Raman, and ^{19}F NMR spectral data of starting modules are reported to show the changes occurring on PFC-HC adduct formation. X-ray crystal structures were determined by using a Bruker P4 diffractometer.

General procedure: **formation of cocrystal 3a made up of 1,4-dibromotetrafluorobenzene (1a) and 4,4′-dipyridyl (2a)**: Equimolar amounts of the dibromoarene **1a** and of the dipyridyl **2a** were dissolved in a vial of clear borosilicate glass at room temperature. Chloroform was used as solvent. The open vial was placed in a closed cylindrical wide-mouth bottle containing vaseline oil. $CHCl_3$ was allowed to diffuse at room temperature and after two days, cocrystal **3a** was obtained as colorless elongated prisms. M.p. (chloroform): 110–115 °C; ^{19}F NMR ($CDCl_3$): pure **1a** (0.80 M): $\delta = -132.32$ ppm; cocrystal **3a** (0.80 M): $\Delta\delta = \delta_{1a} - \delta_{3a} = 0.04$ ppm; FT-IR (KBr pellet, selected bands): pure **1a**: $\tilde{\nu} = 1487, 1450, 990, 957, 790\ cm^{-1}$; pure **2a**: $\tilde{\nu} = 3075, 3046, 3027, 1591, 1407, 989, 807, 608\ cm^{-1}$; cocrystal **3a**: $\tilde{\nu} = 3085, 3050, 3036, 1485, 1480, 1447, 1405, 799, 785\ cm^{-1}$; Raman (neat, selected bands): pure **1a**: $\tilde{\nu} = 1618, 1406, 507, 443, 396, 211, 171\ cm^{-1}$; pure **2a**: $\tilde{\nu} = 3054, 1619, 1607, 1299, 1001\ cm^{-1}$; cocrystal **3a**: $\tilde{\nu} = 3075, 1603, 1288, 1003, 505, 208\ cm^{-1}$; elemental analysis calcd (%) for $C_{16}H_8Br_2F_4N_2$: C 41.41, H 1.74, Br 34.44, N 6.04; found C 41.17, H 2.01, Br 34.65, N 5.83.

Formation of the cocrystal 3b made up of 1,4-dibromotetrafluorobenzene (1a) and (*E*)-1,2-bis(4-pyridyl)ethylene (2b): The procedure described above was used. Analyzed cocrystal **3b** was a colorless amygdule. M.p. (chloroform): 130–135 °C; ^{19}F NMR ($CDCl_3$): cocrystal **3b** (0.44 M): $\Delta\delta = \delta_{1a} - \delta_{3b} = 0.01$ ppm; FT-IR (KBr pellet, selected bands): pure **2b**: $\tilde{\nu} = 3050, 3028, 1596, 1413, 982, 822, 552\ cm^{-1}$; cocrystal **3b**: $\tilde{\nu} = 3058, 3031, 1597, 1478, 1412, 995, 953, 823, 784, 553\ cm^{-1}$; Raman (neat, selected bands): pure **2b**: $\tilde{\nu} = 1641, 1597, 1237, 1198, 996, 123\ cm^{-1}$; cocrystal **3b**: $\tilde{\nu} = 1642, 1597, 1338, 1240, 1200, 998, 208, 120\ cm^{-1}$; elemental analysis calcd (%) for $C_{18}H_{10}Br_2F_4N_2$: C 44.11, H 2.06, Br 32.61, N 5.72; found C 43.89, H 2.23, Br 32.93, N 5.59.

Formation of the cocrystal 3c made up of 1,3-dibromotetrafluorobenzene (1b) and 4,4′-dipyridyl (2a): The procedure described above was used. Cocrystal **3c** was isolated as colorless rhombic prisms. M.p. (chloroform): 65–67 °C; ^{19}F NMR ($CDCl_3$): pure **1b** (0.91 M): $\delta = -103.31$ (1F; F-2), -125.94 (2F; F-3), -160.07 ppm (1F; F-4); cocrystal **3c** (0.91 M): $\Delta\delta = \delta_{1b} - \delta_{3c} = 0.26$ (F-2), 0.27 (F-3), 0.12 (F-4); FT-IR (KBr pellet, selected bands): pure **1b**: $\tilde{\nu} = 1490, 1450, 1085, 897, 743, 701\ cm^{-1}$; cocrystal **3c**: $\tilde{\nu} = 3083, 3050, 1589, 1481, 1450, 1068, 889, 800, 739, 732, 698\ cm^{-1}$.

Formation of the cocrystal 3d made up of 1,3-dibromotetrafluorobenzene (1b) and (*E*)-1,2-bis(4-pyridyl)ethylene (2b): The procedure described above was used. Cocrystal **3d** was isolated as colorless elongated prisms. M.p. (chloroform): 70–73 °C; ^{19}F NMR ($CDCl_3$): cocrystal **3d** (0.91 M): $\Delta\delta = \delta_{1b} - \delta_{3d} = 0.07$ (F-2), 0.09 (F-3), 0.03 ppm (F-4); FT-IR (KBr pellet, selected bands): cocrystal **3d**: $\tilde{\nu} = 3069, 3058, 3034, 1597, 1482, 1068, 993, 890, 740, 697\ cm^{-1}$.

Formation of the cocrystal 3e made up of 1,2-dibromotetrafluorobenzene (1c) and 4,4′-dipyridyl (2a): The procedure described above was used. Cocrystal **3e** was isolated as colorless pseudo-hexagonal prisms. M.p. (chloroform): 62–65 °C; ^{19}F NMR ($CDCl_3$): pure **1c** (0.68 M): $\delta = -125.44$ (F-3), -154.25 ppm (F-4); cocrystal **3e** (0.68 M): $\Delta\delta = \delta_{1c} - \delta_{3e} = 0.19$ (F-3), 0.18 ppm (F-4); FT-IR (KBr pellet, selected bands): pure **1c**: $\tilde{\nu} = 1504, 1464, 1120, 1037, 851, 805\ cm^{-1}$; cocrystal **3e**: $\tilde{\nu} = 3055, 3047, 3031; 1590, 1497, 1463, 1035, 995, 847, 802\ cm^{-1}$; Raman (neat, selected bands): pure **1c**: $\tilde{\nu} = 1617, 1260, 805, 479, 373, 270, 130\ cm^{-1}$; cocrystal **3e**: $\tilde{\nu} = 3069, 1594, 1289, 1235, 1002, 660, 479, 370, 267, 131\ cm^{-1}$.

Formation of the cocrystal 3f made up of 1,2-dibromotetrafluorobenzene (1c) and (*E*)-1,2-bis(4-pyridyl)ethylene (2b): The procedure described above was used and chloroform evaporation was performed at -5 °C. Cocrystal **3f** was isolated as colorless irregular prisms. M.p. (chloroform): 60–64 °C; ^{19}F NMR ($CDCl_3$): cocrystal **3f** (0.68 M): $\Delta\delta = \delta_{1c} - \delta_{3f} = 0.03$ (F-3), 0.02 ppm (F-4); FT-IR (KBr pellet, selected bands): cocrystal **3f**: $\tilde{\nu} = 3034, 1597, 1497, 1463, 1418, 1032, 995, 826, 802\ cm^{-1}$; Raman (neat, selected bands): cocrystal **3b**: $\tilde{\nu} = 1641, 1596, 1340, 1234, 1199, 996, 266, 120\ cm^{-1}$.

Formation of the cocrystal 1a·1,2-BPE made up of 1,4-dibromotetrafluorobenzene (1a) and 1,2-bis(4-pyridyl)ethane (1,2-BPE): The procedure described above was used.[6a] M.p. (chloroform): 109–111 °C; FT-IR (KBr pellet, selected bands): pure 1,2-BPE: $\tilde{\nu} = 3067, 3031, 2860, 1596, 1456, 1414, 991, 828, 547\ cm^{-1}$; cocrystal **1a**·1,2-BPE: $\tilde{\nu} = 3077, 2960, 2868, 1596, 1482, 9934, 954\ 824, 548\ cm^{-1}$.

Formation of the cocrystal 1,4-DITFB·2a made up of 1,4-diiodotetrafluorobenzene (1,4-DITFB) and 4,4′-dipyridyl (2a): The procedure described above was used.[6a] M.p. (chloroform): 180–182 °C; FT-IR (KBr pellet, selected bands): pure 1,4-DITFB: $\tilde{\nu} = 1465, 1214, 943, 760\ cm^{-1}$; cocrystal **2a**·1,4-DITFB: $\tilde{\nu} = 3029, 1592, 1535, 1456, 1218, 1209, 992, 938, 802, 751, 614\ cm^{-1}$; Raman (neat, selected bands): pure 1,4-DITFB: $\tilde{\nu} = 1610, 1384, 500, 159\ cm^{-1}$; 1,4-DITFB·**2a**: $\tilde{\nu} = 3074, 1612, 1598, 1285, 1008, 500, 152, 105\ cm^{-1}$.

Formation of the cocrystal 1,4-DITFB·2b made up of 1,4-diiodotetrafluorobenzene (1,4-DITFB) and (*E*)-1,2-bis(4-pyridyl)ethylene (2b): Co-

crystal **2b**·1,4-DITFB[6a] was obtained in a few minutes as colorless plates by mixing an equimolar solution of the starting materials in chloroform in a vial of clear borosilicate glass at room temperature. M.p. (chloroform): 236–240 °C; FT-IR (KBr pellet, selected bands): cocrystal 1,4-DITFB·**2b**: $\tilde{\nu}$ = 3058, 3035, 1598, 1455, 1199, 971, 938, 822, 749, 543 cm^{-1}; Raman (neat, selected bands): cocrystal 1,4-DITFB·**2b**: $\tilde{\nu}$ = 1640, 1598, 1336, 1239, 1198, 1001, 500, 149, 113 cm^{-1}.

Formation of the cocrystal 1,4-DITFB·1,2-BPE made up of 1,4-diiodotetrafluorobenzene (1,4-DITFB) and 1,2-bis(4-pyridyl)ethane (1,2-BPE): The general procedure described above was used.[6d] M.p. (chloroform): 204–207 °C; FT-IR (KBr pellet, selected bands): cocrystal 1,4-DITFB·1,2-BPE: $\tilde{\nu}$ = 3074, 3036, 2872, 1601, 1455, 1001, 939, 821, 749, 543 cm^{-1}; elemental analysis calcd (%) for $C_{18}H_{12}I_2F_4N_2$: C 36.89, H 2.06, I 43.30, N 4.78; found: C 36.69, H 2.33, I 43.10, N 4.42.

Formation of the cocrystal 1,2-DITFB·2a made up of 1,2-diiodotetrafluorobenzene (1,2-DITFB) and 4,4′-dipyridyl (2a): The general procedure described above was used.[6c] White cocrystals were obtained. M.p. (chloroform): 138–140 °C; FT-IR (KBr pellet, selected bands): pure 1,2-DITFB: $\tilde{\nu}$ = 1494, 1442, 1110, 1024, 815, 773 cm^{-1}; cocrystal 1,2-DITFB·**2a**: $\tilde{\nu}$ = 3041, 1593, 1483, 1429, 1307, 1218, 1009, 811, 612 cm^{-1}; Raman (neat, selected bands): pure 1,2-DITFB: $\tilde{\nu}$ = 1613, 1255, 774, 472, 360, 345, 235, 101 cm^{-1}; cocrystal 1,2-DITFB·**2a**: $\tilde{\nu}$ = 3070, 1599, 1291, 1005, 471, 357, 332, 227, 149 cm^{-1}.

Formation of the cocrystal 1,4-DIB·2a made up of 1,4-diiodobenzene (1,4-DIB) and 4,4′-dipyridyl (2a): The cocrystals[6a] were obtained with the general procedure described above using dichloromethane as solvent. M.p. (dicholoromethane): 147–149 °C; FT-IR (KBr pellet, selected bands): cocrystal 1,4-DIB·**2a**: $\tilde{\nu}$ = 3032, 1587, 1531, 1401, 1373, 1214, 998, 988, 808, 793, 608 cm^{-1}; Raman (neat, selected bands): pure 1,4-DIB: $\tilde{\nu}$ = 3101, 3051, 1550, 1044, 684, 159, 119 cm^{-1}; cocrystal 1,4-DIB·**2a**: $\tilde{\nu}$ = 3051, 1595, 1287, 1231, 1004, 683, 332, 155 cm^{-1}.

Formation of the cocrystal 1,4-DIB·2b made up of 1,4-diiodobenzene (1,4-DIB) and *trans*-1,2-bis(4-pyridyl)ethylene (2b): The cocrystals 1,4-DIB·**2b**[6a] were obtained by the general procedure described above, using dichloromethane as solvent. M.p. (dicholoromethane): 140–142 °C; FT-IR (KBr pellet, selected bands): cocrystal 1,4-DIB·**2b**: $\tilde{\nu}$ = 3070, 3031, 1594, 1412, 1374, 1067, 994, 971, 826, 551 cm^{-1}; Raman (neat, selected bands): cocrystal 1,4-DIB·**2b**: $\tilde{\nu}$ = 3055, 1641 1594, 1337, 1238, 1197, 997, 155 cm^{-1}.

Formation of the cocrystal 1,4-DIB·1,2-BPE made up of 1,4-diiodobenzene (1,4-DIB) and 1,2-bis(4-pyridyl)ethane (1,2-BPE): The general procedure described above was used. M.p. (chloroform): 145–147 °C; FT-IR (KBr pellet, selected bands): pure 1,4-DIB: $\tilde{\nu}$ = 1460, 1371, 1067, 992, 797 cm^{-1}; cocrystal 1,4-DIB·1,2-BPE: $\tilde{\nu}$ = 3070, 2859, 1596, 1466, 1412, 1069, 994, 825, 810, 544 cm^{-1}; elemental analysis calcd (%) for $C_{18}H_{16}I_2N_2$: C 42.05, H 3.14, I 49.36, N 5.45; found: C 41.88, H 3.31, I 49.05, N 5.22.

General procedure of selective supramolecular syntheses: formation of cocrystal 1,4-DITFB·2a made up of 1,4-diiodotetrafluorobenzene (1,4-DITFB) and 4,4′-dipyridyl (2a): Equimolar amounts of the dibromobenzene **1a**, the diiodobenzene 1,4-DITFB, and the dipyridyl derivative **2a** were dissolved in a vial of clear borosilicate glass at room temperature. Chloroform was used as solvent. The open vial was placed in a closed cylindrical wide-mouth bottle containing vaseline oil. $CHCl_3$ was allowed to diffuse at room temperature and after a few hours the cocrystal 1,4-DITF·**2a** was obtained in pure form (GC and ^{19}F NMR analyses).

Selective supramolecular synthesis of cocrystal 1,4-DITFB·2b made up of 1,4-diiodotetrafluorobenzene (1,4-DITFB) and (*E*)-1,2-bis(4-pyridyl)ethylene (2b): The procedure described above was used. The starting solution was prepared with equimolar amounts of the dibromobenzene **1a**, the diiodobenzene 1,4-DITFB, and the dipyridyl derivative **2b**. The noncovalent cocrystal 1,4-DITFB·**2b** was obtained in pure form (GC and ^{19}F NMR analyses).

Selective supramolecular synthesis of cocrystal 1,2-DITFB·2a made up of 1,2-diiodotetrafluorobenzene (1,2-DITFB) and 4,4′-dipyridyl (2a): The general procedure was used. The starting solution was prepared with equimolar amounts of the dibromobenzene **1c**, the diiodobenzene 1,2-DITFB, and the dipyridyl derivative **2a**. The noncovalent cocrystal 1,2-DITFB·**2a** was obtained in pure form (GC and ^{19}F NMR analyses).

Selective supramolecular synthesis of cocrystal 1,2-DITFB·2b made up of 1,2-diiodotetrafluorobenzene (1,2-DITFB) and (*E*)-1,2-bis(4-pyridyl)ethylene (2b): The general procedure described above was used. The starting solution was prepared with equimolar amounts of the dibromobenzene **1c**, the diiodobenzene 1,2-DITFB, and the dipyridyl derivative **2b**. The noncovalent cocrystal 1,2-DITFB·**2b** was obtained in pure form (GC and ^{19}F NMR analyses).

Selective supramolecular synthesis of cocrystal 1,4-DIB·2b made up of 1,4-diiodobenzene (1,4-DIB) and (*E*)-1,2-bis(4-pyridyl)ethylene (2b): The general procedure was used. The starting solution was prepared with equimolar amounts of the dibromobenzene **1a**, the diiodobenzene 1,4-DIB, and the dipyridyl derivative **2b**. At 30% recovery of **2b**, a 75:25 mixture of the noncovalent cocrystals 1,4-DIB·**2b** and **3b** was obtained (GC and ^{19}F/^{1}H NMR analyses). Two further recrystallizations of this enriched mixture afforded 1,4-DIB·**2b** in pure form.

Selective supramolecular synthesis of cocrystal 3b made up of 1,4-dibromotetrafluorobenzene (1a) and (*E*)-1,2-bis(4-pyridyl)ethylene (2b): The general procedure was used. The starting solution was prepared with equimolar amounts of the two dibromobenzenes **1a** and **1b**, and the dipyridyl derivative **2b**. The copolymer **3b** was obtained in pure form after one day. A second selective formation of the same cocrystal **3b** has been realized by using the procedure described above, but a different starting solution was employed. Equimolar amounts of the two dibromobenzenes **1a** and **1c**, and the dipyridyl derivative **2b** were crystallized as usual. The cocrystal **3b** was obtained in pure form after one day (GC and ^{19}F NMR analyses).

Selective supramolecular synthesis of 3e made of 1,2-dibromotetrafluorobenzene (1c) and dipyridyl (2a): The general procedure was used. The starting solution was prepared with equimolar amounts of the dibromobenzenes **1b** and **1c**, and the dipyridyl **2a**. At 35% recovery of **2a**, an 80:20 mixture of the noncovalent cocrystals **3e** and **3c** was obtained (GC and ^{19}F NMR analyses). One further recrystallization of this enriched mixture afforded **3e** in pure form.

Single-crystal X-ray analyses: Data were collected with a Bruker APEX CCD area detector diffractometer, equipped with a Bruker KRIOFLEX low-temperature device, using $Mo_{K\alpha}$ radiation (λ = 0.71069 Å), graphite monochromator, ω and ϕ scans; the temperature was fixed at 90 K and during the experiments its variation was in the range of $\pm$0.1°, but on the basis of the calibration curve hysteresis we evaluate the temperature standard deviation to be at least 2°; data collection and data reduction were performed by SMART and SAINT, and the absorption correction, based on multiscan procedure, by SADABS.[33] The structures were solved by SIR 92,[34] and refined on all independent reflections by full-matrix least-squares based on F_o^2 using SHELX-97.[35] For **3a**, **3b**, **3e**, and **3f**, heavy atoms were anisotropic and H atoms isotropic and fully refined; for **3c**, H atoms ADPs were constrained to be 1.2 times the isotropic ADP of the connected C atoms; only in the case of **3d**, in which the **2b** molecule is disordered, N and C atoms with a reduced separation were treated isotropically and H atoms were calculated. Moreover, to reduce the parameters' correlation, the same geometric restraints were adopted for this molecule. CCDC-199297 (**3a**), CCDC-199292 (**3b**), CCDC-199295 (**3c**), CCDC-199294 (**3d**), CCDC-199296 (**3e**), and CCDC-199293 (**3f**) contain the supplementary crystallographic data for this paper. These data can be obtained free of charge via www.ccdc.can.ac.uk/conts/retrieving.html (or from the Cambridge Crystallographic Center, 12 Union Road, Cambridge CB2 1EZ, UK; Fax: (+44) 1223-336033; or deposit@ccdc.cam.ac.uk).

Acknowledgement

The European Union (RTN contract HPRN-CT-2000-00002) and Miur (Cofinanziamento 2001 and FIRB "Interazioni deboli") are gratefully acknowledged for financial support.

[1] a) B. E. Smart in *Organofluorine Chemistry: Principles and Commercial Applications*, (Eds.: R. E. Banks, B. E. Smart, J. C. Tatlow), Plenum Press, New York, **1994**, pp. 57–82; b) J. Hildebrand, D. R. F. Cochran, *J. Am. Chem. Soc.* **1949**, *71*, 22–25; c) D. L. Dorset, *Macromolecules* **1990**, *23*, 894–901.

[2] a) J. H. Williams, *Acc. Chem. Res.* **1993**, *26*, 593–598; b) G. W. Coates, D. A. Dougherty, A. R. Dunn, R. H. Grubbs, L. M. Henling, *Angew.*

Chem. **1997**, *109*, 290–293; *Angew. Chem. Int. Ed.* **1997**, *36*, 248–251; c) F. Cozzi, F. Ponzini, R. Annunziata, M. Cinquini, Y. S. Siegel, *Angew. Chem.* **1995**, *107*, 1092–1093; *Angew. Chem. Int. Ed.* **1995**, *34*, 1019–1020; d) H. Adams, J.-L. J. Blanco, G. Chessari, C. A. Hunter, C. M. R. Low, J. M. Sanderson, J. R. Vinter, *Chem. Eur. J.* **2001**, *7*, 3494–3503.

[3] a) O. Hassel, *Science* **1970**, *170*, 497–502; b) J. M. Dumas, L. Gomel, M. Guerin in *The Chemistry of Functional Groups, Supplement D* (Eds.: S. Patai, Z. Rappoport), Wiley, New York, **1983**, pp. 985–1020; c) H. A. Bent, *Chem. Rev.* **1968**, *68*, 587–648; d) A. C. Legon, *Chem. Eur. J.* **1998**, *4*, 1890–1897; e) A. C. Legon, *Angew. Chem.* **1999**, *111*, 2850–2880; *Angew. Chem. Int. Ed.* **1999**, *38*, 2687–2714; f) G. R. Desiraju, R. L. Harlow, *J. Am. Chem. Soc.* **1989**, *111*, 6757–6764.

[4] a) J. P. M. Lommerse, A. J. Stone, R. Taylor, F. H. Allen, *J. Am. Chem. Soc.* **1996**, *118*, 3108–3116; b) N. Ramasubbu, R. Parthasarathy, P. Murray-Rust, *J. Am. Chem. Soc.* **1986**, *108*, 4308–4314.

[5] B. Améduri, B. Boutevin, *J. Fluor. Chem.* **1999**, *100*, 97–116.

[6] a) R. B. Walsh, C. W. Padgett, P. Metrangolo, G. Resnati, T. W. Hanks, W. T. Pennington, *Cryst. Growth Des.* **2001**, *1*, 165–175; b) M. T. Messina, P. Metrangolo, W. Panzeri, T. Pilati, G. Resnati, *Tetrahedron* **2001**, *57*, 8543–8550; c) R. Liantonio, P. Metrangolo, T. Pilati, G. Resnati, *Acta Crystallogr. Sect. E* **2002**, *58*, 575–577; d) E. Corradi, S. V. Meille, M. T. Messina, P. Metrangolo, G. Resnati, *Angew. Chem.* **2000**, 112, 1852–1856; *Angew. Chem. Int. Ed.* **2000**, *39*, 1782–1786; e) R. Liantonio, S. Luzzati, P. Metrangolo, T. Pilati, G. Resnati, *Tetrahedron* **2002**, *58*, 4023–4029.

[7] a) R. N. Haszeldine, *J. Chem. Soc.* **1953**, 2622–2626; b) R. Weiss, O. Schwab, F. Hampel, *Chem. Eur. J.* **1999**, *5*, 968–974; c) R. Weiss, G.-E. Miess, A. Haller, W. Reinhardt, *Angew. Chem.* **1986**, 98, 102–103; *Angew. Chem. Int. Ed.* **1986**, *25*, 103–104.

[8] G. Valerio, G. Raos, S. V. Meille, P. Metrangolo, G. Resnati, *J. Phys. Chem. A* **1999**, *104*, 1617–1620.

[9] a) N. F. Cheetham, I. J. McNaught, A. D. E. Pullin, *Aust. J. Chem.* **1974**, *27*, 973–985; b) S. Akyüz, *J. Mol. Struct.* **1998**, *449*, 23–27; c) B. Brzezinski, G. Zundel, *Can. J. Chem.* **1981**, *59*, 786–794; d) J. R. McDivitt, G. L. Humphrey, *Spectrochim. Acta* **1974**, *30A*, 1021–1033.

[10] R. Foster, *Organic Charge-Transfer Complexes*, Academic Press, London, **1969**, pp. 100–103.

[11] a) J. N. Gayles, *J. Chem. Phys.* **1968**, *49*, 1840–1847; b) R. A. Zingaro, W. E. Tolberg, *J. Am. Chem. Soc.* **1959**, *81*, 1353–1357; c) K. Yokobayashi, F. Watari, K. Aida, *Spectrochim. Acta* **1968**, *24A*, 1651–1655.

[12] a) R. Bertani, P. Metrangolo, A. Moiana, E. Perez, T. Pilati, G. Resnati, I. RicoLattes, A. Sassi, *Adv. Mater.* **2002**, *14*, 1197–1201; b) A. De Santis, R. Liantonio, T. A. Logothetis, M. T. Messina, P. Metrangolo, G. Resnati, *Coll. Czech. Chem. Commun.* **2002**, *67*, 1373–1382; c) C. Guardigli, R. Liantonio, M. L. Mele, P. Metrangolo, G. Resnati, *Supramol. Chem.* **2003**, *15*, 177–188; d) D. D. Burton, F. Fontana, P. Metrangolo, T. Pilati, G. Resnati, *Tetrahedron Lett.* **2003**, *44*, 645–648.

[13] a) J. Roukolainen, J. R. Tanner, G. ten Brinke, E. L. Thomas, O. Ikkala, *Macromolecules* **1998**, *31*, 3532–3536; b) J. Roukolainen, M. Saariaho, R. Serimaa, G. ten Brinke, E. L. Thomas, O. Ikkala, *Macromolecules* **1999**, *32*, 1152–1158.

[14] A. Bondi, *J. Phys. Chem.* **1964**, *68*, 441–451.

[15] F. Fontana, A. Forni, P. Metrangolo, W. Panzeri, T. Pilati, G. Resnati, *Supramol. Chem.* **2002**, *14*, 47–55.

[16] a) C. J. Brown, *Acta Crystallogr.* **1966**, *21*, 153–158; b) A. Hoekstra, P. Meertens, A. Vos, *Acta Crystallogr. Sect. B* **1975**, *31*, 2813–2817; c) G. Casalone, T. Pilati, M. Simonetta, *Tetrahedron Lett.* **1980**, *21*, 2345–2348.

[17] a) T. Messina, P. Metrangolo, W. Panzeri, E. Ragg, G. Resnati, *Tetrahedron Lett.* **1998**, *39*, 9069–9072; b) P. Metrangolo, W. Panzeri, F. Recupero, G. Resnati, *J. Fluor. Chem.* **2002**, *114*, 27–33.

[18] a) M. Fujita in *Molecular Catenanes, Rotaxanes and Knots: A Journey through the World of Molecular Topology*, (Eds.: J.-P. Sauvage, C. D. Buchecker), Wiley-VCH, Weinheim, **1999**, pp. 57–76; b) J.-P. Sauvage, M. W. Hosseini in *Comprehensive Supramolecular Chemistry, Vol. 9* (Eds.: J. L. Atwood, J. E. Davies, D. D. MacNicol, E. Vögtle), Elsevier, Oxford, **1996**, pp. 10, 259, 261, and 302; c) A. N. Khlobystov, A. J. Blake, N. R. Champness, D. A. Lemenovskii, A. G. Majouga, N. V. Zyk, M. Schröder, *Coord. Chem. Rev.* **2001**, *111*, 155–192.

[19] a) L. R. MacGillivray, J. L. Reid, J. A. Ripmeester, *J. Am. Chem. Soc.* **2000**, *122*, 7817–7818; b) G. S. Papaesfstathiou, L. R. MacGillvray, *Org. Lett.* **2000**, *3*, 3835–3838; c) G. S. Papaefstathiou, A. J. Kipp, L. R. MacGillivray, *Chem. Commun.* **2001**, 2462–2463; d) J. A. Cowan, J. A. K. Howard, M. A. Leech, *Acta Crystallogr. Sect. C* **2001**, *57*, 1196–1198; e) M. B. Zaman, M. Tomura, Y. Yamashita, *J. Org. Chem.* **2001**, *66*, 5987–5995.

[20] a) M. Simard, D. Su, J. D. Wuest, *J. Am. Chem. Soc.* **1991**, *113*, 4696–4698; b) D. Su, X. Wang., M. Simard, J. D. Wuest, *Supramol. Chem.* **1995**, *6*, 171–178.

[21] a) P. L. Wash, S. Ma, U. Obst, J. Rebek, *J. Am. Chem. Soc.* **1999**, *121*, 7973–7974; b) J. M. Dumas, C. Geron, A. M. Khribii, M. Lakraimi, *Can. J. Chem.* **1984**, *62*, 2634–2640; c) R. C. Castell, A. M. Nardillo, *J. Solution Chem.* **1985**, *14*, 87–100; d) M. F. Budyka, T. N. Gavrishova, O. D. Laukhina, E. M. Koldasheva, *Izv. Akad. Nauk. Ser. Khim.* **1995**, *10*, 1725–1730 (*Russ. Chem. Bl.* **1995**, *44*, 1656–1661); e) T. Okuda, T. Suzuki, H. Negita, *J. Mol. Struct.* **1983**, *111*, 177–182; f) G. Kozakowski, *Pol. J. Chem.* **1984**, *58*, 487–495; g) J. F. Bertran, M. Rodriguez, *Org. Magnetic Res.* **1979**, *12*, 92–94.

[22] a) S. C. Blackstock, J. K. Kochi, *J. Org. Chem.* **1987**, *52*, 1451–1460; b) S. C. Blackstock, J. K. Kochi, *J. Am. Chem. Soc.* **1987**, *109*, 2484–2496.

[23] S. A. Cooke, G. Cotti, G. M. Evans, J. H. Halloway, Z. Kisiel, A. C. Legon, J. M. A. Thumwood, *Chem. Eur. J.* **2001**, *7*, 2295–2305.

[24] T. Dahl, O. Hassel, *Acta Chem. Scand.* **1968**, *22*, 2851–2866.

[25] T. Dahl, O. Hassel, *Acta Chem. Scand.* **1971**, *25*, 2168–2174.

[26] a) P. Kronebusch, W. B. Gleson, D. Britton, *Cryst. Struct. Commun.* **1976**, *5*, 17–20; b) G. B. Ansell, *J. Chem. Soc. Perkin Trans. 2* **1973**, 2036–2038; c) J. R. Witt, D. Britton, C. Mahon, *Acta Crystallogr. Sect. B* **1972**, *28*, 950–955; d) J. Silverman, A. P. Krukonis, N. F. Yannoni, *Acta Crystallogr. Sect. B* **1973**, *29*, 2022–2024; e) H. Noerenberg, H. Kratzin, P. Boldt, W. S. Sheldrick, *Chem. Ber.* **1977**, *110*, 1284–1293; f) E. Gunther, S. Hunig, J.-U. von Schutz, U. Langohr, H. Rieder, S. Soderholm, H.-P. Werner, K. Peters, H. G. von Schnering, H. J. Lindner, *Chem. Ber.* **1992**, *125*, 1919–1926; g) V. Figala, T. Gessner, R. Gompper, E. Hadicke, S. Lensky, *Tetrahedron Lett.* **1993**, *34*, 6375–6378; h) E. Gunther, S. Hunig, K. Peters, H. Rieder, H. G. von Schnering, J.-U. von Schutz, S. Soderholm, H. -P. Werner, H. C. Wolf, *Angew. Chem.* **1990**, *102*, 220; *Angew. Chem. Int. Ed.* **1990**, *29*, 204–205. i) H. Ishida, K. Yui, Y. Aso, T. Otsubo, F. Ogura, *Bull. Chem. Soc. Jpn.* **1990**, *63*, 2828–2835.

[27] D. Su, X. Wang, M. Simard, J. D. Wuest, *Supramol. Chem.* **1995**, *6*, 171–178.

[28] C. Wakselman, A. Lantz in *Organofluorine Chemistry: Principles and Commercial Applications*, (Eds.: R. E. Banks, B. E. Smart, J. C. E. Tatlow), Plenum Press, New York, **1994**.

[29] a) R. D. Bailey, M. Grabarczyk, T. W. Hanks, W. T. Pennington, *J. Chem. Soc. Perkin Trans. 2* **1997**, 2781–2786; b) R. D. Bailey, D. Phelps, A. Crihfield, J. Hartwell, T. W. Hanks, W. T. Pennington, *Mol. Cryst. Liq. Cryst.* **2000**, *354*, 1111–1115.

[30] a) M. M. Sedensky, H. F. Cascorbi, J. Meinwald, P. Radford, P. G. Morgan, *Proc. Natl. Acad. Sci. USA* **1994**, *91*, 10054; b) M. M. Sedensky, H. F. Cascorbi, J. Meinwald, P. Radford, P. G. Morgan, *Prog. Anesth. Mech.* **1995**, 220 (*Chem. Abstr.* **1997**, *124*, 106260).

[31] a) R. Matthew, *Science* **1992**, *255*, 156; b) R. Eckenhoff, J. S. Johanson, *Pharmacol. Rev.* **1997**, *49*, 343; c) N. P. Franks, W. R. Lieb, *Nature* **1994**, *367*, 607; d) P. G. Morgan, M. F. Usiak, M. M. Sedensky, *Anaesthesiology* **1996**, *85*, 385.

[32] a) A. Farina, S. V. Meille, M. T. Messina, P. Metrangolo, G. Resnati, G. Vecchio, *Angew. Chem.* **1999**, *111*, 2585–2588; *Angew. Chem. Int. Ed.* **1999**, *38*, 2433–2436; b) *Chem. Eng. News* **1999**, *77(33 August 16)*, 32.

[33] SMART, SAINT and SADABS, Bruker AXS Inc., Madison, Wisconsin, USA, **1999**.

[34] A. Altomare, G. Cascarano, C. Giacovazzo, A. Guagliardi, M. C. Burla, G. Polidori, M. Camalli, *J. Appl. Crystallogr.* **1994**, *27*, 435.

[35] G. M. Sheldrick, SHELXL 97 Program for the Refinement of Crystal Structures, **1997**, University of Göttingen, Germany.

Received: December 10, 2002
Revised: April 7, 2003 [F4655]

